Transportation Research Part C 172 (2025) 105021

Contents lists available at ScienceDirect

Transportation Research Part C

journal homepage: www.elsevier.com/locate/trc

Novel pavement crack detection sensor using coordinated mobile robots

Mohammad Alkhedher [a,*], Abdullah Alsit [a], Marah Alhalabi [b], Sharaf AlKheder [c], Abdalla Gad [b], Mohammed Ghazal [b]

[a] Mechanical Engineering Department, College of Engineering, Abu Dhabi University, Abu Dhabi, 59911, United Arab Emirates

[b] Electrical, Computer, and Biomedical Engineering Department, College of Engineering, Abu Dhabi University, Abu Dhabi, 59911, United Arab Emirates

[c] Civil Engineering Department, College of Engineering and Petroleum, Kuwait University, Safat, 5969, Kuwait

ARTICLE INFO

Keywords:
Pavement crack detection
Road irregularities
Coordinated mobile robots
Sensing technologies
Unmanned aerial vehicle
Unmanned ground vehicle
Autonomous inspection
Image processing

ABSTRACT

This paper proposes a novel pavement crack detection sensor using coordinated mobile robots. The comfort of drivers and the economic efficiency are negatively affected by pavement deterioration due to weather and constant vehicle use. Our proposed system consists of a drone and an unmanned ground robot that checks the quality of roads and shows where cracks and other problems are by measuring and reporting all kinds of irregularities in road surfaces in an autonomous manner. The design of our system is a one-of-a-kind dual-cart unmanned ground vehicle, with its first cart being a drone-mounting body. The drone is equipped with a high-resolution camera for the inspection of roads, cracks, and anomalies remotely using image processing and artificial intelligence. In the event that a crack is identified, a signal is sent to the robot, instructing it to carry out a more comprehensive crack inspection. This inspection involves the use of close-range laser depth and thermal cameras to generate the pavement cracks' depth maps accurately. We incorporate a drone into our proposed coordinated mobile robots system to enable cheaper operations and provide aerial coverage, preventing traffic congestion. Our novel pavement crack detection sensor can be incorporated with governmental agencies such as the Ministry of Transportation, the Municipality, and Civil Defence entities. Pavement and road health surveys can be completed in over fifty percent less time using our coordinated mobile robots system.

1. Introduction

Road inspection and pavement condition assessment are highly interesting to several governmental authorities today. These tasks are frequently accomplished using traditional and manual inspection methods. Several systems have recently been proposed to automate the measurement of road anomalies. However, these systems have been proposed in certain road areas requiring expert testing. There is a crucial need for automated systems that can improve the detection and quantification of pavement defects. In this work, we focus on developing technology capable of identifying visible cracks, which are key indicators of pavement deterioration. These defects will be assessed visually and by measuring their depth using advanced imaging technologies. This approach not only enhances the accuracy of inspections but also significantly speeds up the assessment process by enabling the quick scanning

* Corresponding author.
E-mail addresses: mohammad.alkhedher@adu.ac.ae (M. Alkhedher), 1062242@adu.ac.ae (A. Alsit), marah.alhalabi@adu.ac.ae (M. Alhalabi), sharaf.alkehder@ku.edu.kw (S. AlKheder), abdalla.gad@adu.ac.ae (A. Gad), mohammed.ghazal@adu.ac.ae (M. Ghazal).

https://doi.org/10.1016/j.trc.2025.105021
Received 7 May 2024; Received in revised form 8 January 2025; Accepted 21 January 2025
Available online 7 February 2025
0968-090X/

of large areas and providing real-time data to pavement management systems. Four performance indicators are typically used to indicate pavement deterioration: the International Roughness Index (IRI), the surface modulus, the rut depth, and the friction coefficient (Singh et al., 2018).

Road quality evaluation is a significant concern for many countries. Nowadays, some tests are partially automated using noninvasive techniques such as signal and image processing to reduce the need for human intervention (Harikrishnan and Gopi, 2017; Aleadelat et al., 2018; Zeng et al., 2017; Li et al., 2019; Nguyen et al., 2019; Ciampoli et al., 2019). These new technologies are safer, more efficient, and less costly. The new sensing systems use ground-penetrating radar (Sun et al., 2019; Lai et al., 2018; Ciampoli et al., 2019), ultrasonic (Sharma et al., 2020; Choi and Park, 2019), electro-resistivity (Aygun et al., 2020), or laser technology (Soilán et al., 2019; Zhong et al., 2020). Developing a comprehensive methodology for autonomously evaluating road conditions and pavement deterioration has been a major focus of research. Repetitive traffic loading causes cracks in major highways and typical streets' paving. Typically, repairing these types of cracks takes a significant amount of time. System limitations create a significant gap and difficulties scanning the entire street for other cracks.

Furthermore, building this system comes at a very high cost and many limitations. Commercially available road inspection systems are costly, time-consuming, and require a high experience level. Currently used pavement inspection systems include the following: (1) a crack detection system that automates the detection of road cracks and features (Chun et al., 2021), (2) a digital imaging system for visually identifying and locating deterioration and cracking (Pan et al., 2016), and (3) a geometry system for collecting road geometry and navigation data (Cantisani and Del Serrone, 2020).

After acquiring pavement images to monitor the deterioration of the asphalt concrete pavement caused by aged asphalt material, these images can be analyzed to obtain quantitative values for assessing the pavement's deterioration. However, image resolution has an impact on spectral signal analysis and adds significant uncertainty to the analysis of road or bridge conditions (Pan et al., 2016).

Other recent road inspection technologies include the measurement of asphalt and granular thickness. Over time, asphalt and granular road layers can develop defects such as moisture ingress, compaction failures, and uneven thickness, leading to structural impairments like potholes and cracks. Inspecting these layers for uniformity and internal defects has traditionally been challenging and disruptive, often requiring core drilling, which is time-consuming and damages the road. Ground-penetrating radar (GPR) offers a noninvasive and efficient alternative (Koohmishi et al., 2024). This technology uses radio waves to probe subsurface layers, capturing reflected signals that vary with material properties and boundaries and generating real-time, comprehensive 3D images of the road structure. GPR enables rapid assessments of pavement integrity, detecting anomalies such as uneven thicknesses, voids, and moisture pockets without physical damage.

GPR was discovered to be effective at identifying local construction hazards, allowing for decision-making regarding maintenance and repair plans. Regular and detailed inspections require more specialized equipment, including materials characterization, monitoring systems, remaining life, risk, and cost analysis. These systems are expensive and require ongoing expert monitoring in real-time experiments (Nichols et al., 2017; Garg and Misra, 2020). Real-time non-destructive testing of asphalt density is carried out with the help of PaveScan RDM, which provides precise real-time assessment of pavement quality (Torbaghan et al., 2020). Another recently developed inspection system for pavement assessment is the Quality Inspection and Assessment Robot (QuicaBot). This robot uses cameras and laser scanners to inspect the space for cracks, alignments, hollowness, unevenness, and inclination (Yan et al., 2019).

Other systems use the Morphological Method (Morph), which employs a series of steps to detect cracks accurately. The first step is pre-processing the images of the pavement. This can significantly reduce the impact of pavement texture on the results while also improving the contrast between the concrete pavement and the identified crack. Following that, binarization via thresholding is conducted. This is followed by refinement through closing and, finally, segmentation through shape analysis. The final step is to extract the crack characteristics (Chambon and Moliard, 2011).

According to Josef Stryk and Michal Jank's research (u and Stryk, 2017), cracks can be detected using a thermal camera mounted on the top of the van. A laptop inside the vehicle also monitors the camera system. The test was conducted on rural and urban asphalt roads. Due to the temperature contrast between the cracks on the road, they could be recorded. Because of solar radiation, the temperature of the asphalt road changes, and the surrounding temperature and cracks have an impact on heat transfer in the road. However, accurate measurement appears in the summer, when it is sunny and the road surface has a higher temperature. According to the research study, Taiwan's unusually high prevalence of street maintenance holes results in cracks in the road pavements. The temperature distribution of the cracked concrete was monitored using infrared thermal imaging technology. Thermal imaging is a procedure based on the standard that temperatures above absolute zero allow for the emission of infrared energy. Additionally, the more infrared energy radiation an object emits, the hotter it is. This technology enables rapid temperature measurement and visual observation of temperature distribution (Chen et al., 2013).

The current trend in UGV-based pavement testing is mainly limited to several factors, such as the use of a single crack detection technique (Rahman et al., 2021a,b; Lin et al., 2021), limitations in the mobility of the UGV (Rahman et al., 2021a; Ramalingam et al., 2021; Merkle et al., 2020), and a relatively long time in the crack detection process (Ramalingam et al., 2021). Authors of Rahman et al. (2021a) present an unmanned track maintenance system called a Robotic Inspection and Repair System (RIRS). Such a system achieves navigation and inspection of the tracks and road pavements and performs on-track inspection and repair using a UGV (Rahman et al., 2021a,b). In other applications, UGVs are utilized to distinguish pavements from other objects. For instance, pavement flaws are detected and localized using a Deep Convolutional Neural Network (DCNN)-based object detection system as well semantic segmentation framework SegNet (Ramalingam et al., 2021; Merkle et al., 2020). Moreover, UGV is used to avoid and resist pavement cracks by applying a robust approach for vision-aided inertial navigation and improving the unscented

Kalman filter (Zhai et al., 2021; Lin et al., 2021). To the best of our knowledge, our system is more comprehensive than the current UGV systems in terms of speed in detecting cracks with high efficiency as it includes a vehicle and a drone that works consistently and this will give the device better mobility. Also, use several techniques and sensors to detect cracks such as relying on the thermal camera and the depth camera.

Structural Health Monitoring (SHM) procedures are critical in managing infrastructures, including highways, bridges, and pavements. Asphalt concrete pavements are primarily utilized for roads and bridges. However, such pavements may have numerous cracks due to shrinkage and creep. Inspecting these cracks reliably and efficiently is particularly important for road and bridge structures (Prasanna et al., 2016). Our proposed framework leverages advancements in sensor technology, including laser depth cameras, to provide authorities with an advanced integrated system for scanning road surfaces. This technology enables the detection of surface anomalies and obstacles and the precise measurement of crack depths. By determining how deep a crack extends beneath the surface, our system helps assess the damage's severity and informs the necessary maintenance actions. This depth-specific data is crucial for deciding the appropriate intervention, routine maintenance, or more comprehensive measures, thereby enhancing the robustness and efficacy of the SHM process.

Several studies have explored three-dimensional (3D) crack detection using point cloud data. For instance, one method combines an improved sliding window algorithm with random sample consensus (RANSAC) to extract cracks, while another approach transforms point cloud data into 2D images for automatic crack detection using YOLOv5, which effectively detects pavement cracks with minimal noise (Dong et al., 2023). A similar focus on 3D crack detection is presented in other research that utilizes an autonomous multiscale clustering model to classify irregular cracks like linear and netted types. The system achieves high precision across various crack categories and is crucial for extending the service life of pavement through better maintenance decisions (Lang et al., 2020).

The application of deep learning for crack detection is another prevalent theme. One paper proposes a two-stage framework that uses convolutional neural networks (CNN) and a separation-combination strategy coupled with Crack Transformer v2 (CTv2) to detect pavement surface cracks at the pixel level (Guo et al., 2024). Meanwhile, an improved lightweight semantic segmentation model based on BiSeNetv2 integrates low-level details and high-level semantic context for crack detection. This model demonstrates superior performance in segmentation accuracy, outperforming other methods with a 10.14% improvement in the F1 score (Yu et al., 2024).

Transformer-based models also show promise in this field. The Swin-Unet model, which improves upon the Swin-Unet architecture, utilizes a skip attention module and residual Swin Transformer blocks to enhance crack detection performance. This method captures critical crack features, yielding higher mF1, mPrecision, and mRecall scores compared to existing models like Swin-Unet and Unet (Chen et al., 2024).

In contrast, infrared thermography has been proposed as a cost-effective non-intrusive testing method for detecting surface and near-surface distresses, such as pavement cracks. A study developed an integrated system combining infrared and high-resolution visual imaging with real-time processing to detect and assess cracks' severity. This system effectively correlated surface temperature gradients with crack depth, enhancing decision-making for pavement preservation (Golrokh et al., 2021). The GSkYOLOv5 model further advances infrared-based detection by improving feature learning through GhostNet and Selective Kernel Networks, achieving better performance compared to YOLOv5s (Jiang et al., 2024).

Table 1 lists the technical aspects of pavement crack detection methods from the literature.

This paper proposes a comprehensive autonomous system that integrates multiple functions for scanning large areas of road pavement with an inspection drone that uses a camera with real-time image analysis to detect any pavement anomalies. An Unmanned Ground Vehicle (UGV) equipped with multiple sensing elements is used to conduct a thorough inspection and detection, accurately measuring pavement deficiencies and classifying them using an AI-powered classification and recognition system. The contribution of this paper compared to existing solutions lies in (1) proposing an autonomous system for crack detection in pavement structures using coordinated mobile robots consisting of a UGV with an accompanying drone for guidance, (2) implementing a two-step procedure utilizing drone-acquired images for initial crack detection followed by UGV thorough inspection, and (3) eliminating the need for additional technical people's inspection of crack detection while helping in cutting their survey cost by nearly 50%. Such contributions highlight the research significance of our work in advancing knowledge in the design and implementation of end-to-end multi-robot systems, proposing a new crack detection technique that improves upon the one in the popular CrackIT method, automating the process of road inspections and, in doing so increasing its safety and reducing its cost.

The remainder of the paper is organized in the following manner. The system and methodology of our proposed research work are presented in Section 2, while the results of our proposed system are discussed in Section 3. In Section 5, we conclude our work.

2. Materials and methods

We propose an integrated unmanned ground vehicle-drone system. The unmanned ground vehicle (UGV) is designed to conduct a detailed scan of the area of interest identified by the surveillance drone. The expected outcomes will aid authorities in real-time monitoring of road obstacles and pavement deterioration. This system will therefore attract local transportation, municipality, and airport authorities.

The primary function of an associated drone is to conduct an initial visual inspection and identify significant areas of cracking by scanning large sections of a road or bridge deck (Lei et al., 2018). The drone is programmed to use image analysis techniques to estimate the crack's width and length (Dorafshan et al., 2019). The proposed drone is equipped with imaging capabilities to detect road irregularities. Image binarization is applied to the crack image to detect its dimensions (Kim et al., 2017).

Table 1
Technical aspects of pavement crack detection methods.

Method	Algorithm type	Input data type
Improved Sliding Window with RANSAC (Dong et al., 2023)	Sliding window combined with RANSAC for 3D crack extraction	3D point cloud data
YOLOv5 with Point Cloud Images (Dong et al., 2023)	YOLOv5 applied to 2D images transformed from point cloud data	2D images derived from 3D point cloud
CNN + CTv2 (Guo et al., 2024)	CNN for initial image classification and Crack Transformer v2 (CTv2) for pixel-level detection	High-resolution CCD camera images
BiSeNetv2 (Yu et al., 2024)	Lightweight semantic segmentation (BiSeNetv2) with a guided aggregation module	2D pavement surface images
Swin-Unet (Chen et al., 2024)	Swin-Unet with skip attention and residual Swin Transformer blocks	Public benchmark datasets (CFD, Crack500, CrackSC)
Multiscale Clustering (Lang et al., 2020)	Multiscale clustering and minimum circumscribed rectangle for crack characterization	3D pavement surface images
Infrared Imaging + Thermal Processing (Golrokh et al., 2021)	Combines thermal and visual image processing with correlation analysis	Infrared and visual images
GSkYOLOv5 (Jiang et al., 2024)	GSkYOLOv5 with GhostNet and Selective Kernel Networks for feature enhancement	Infrared images of pavement cracks

2.1. System operation

The mobile UGV's primary purpose is to conduct crack detection analysis on a road or bridge in preparation for maintenance. This system will allow for a more thorough inspection and detection of cracks than a human eye, which can be detected even before the crack is visible on the inspected road. Initially, the UGV uses a high-resolution camera to capture images. A laser sensor mounted on the vehicle generates a two-dimensional map of the study area. The UGV will create a 2D navigation map to locate the inspected cracks' relative position and store these measurements in a map-based database. This map will assist in identifying the UGV and identifying areas where the UGV has not yet performed the crack inspection. The data collected is wirelessly transmitted to the camera's main station. The crack detection system will then proceed to the final step, image processing via the main computer. Cracks can be detected and located on the generated two-dimensional map (Lim et al., 2011).

Fig. 1 depicts the system architecture's block diagram, which explains the implemented process for detecting and processing crack parameters in road pavements. The UAV does a surveying flight covering a wider area quickly identifying location to potential cracks without needing to be accurate or precise. The locations identified by the UAV are then inserted as waypoints and used by the Dijkstra's algorithm to create the UGV path. The UGV follows the path to detect and assess the cracks slowly, accurately, and precisely. Once detected, the thermal and depth cameras are used to collect additional imaging data that can be used later to further characterize and study the cracks. UGV motors are controlled using LabVIEW and MATLAB to perform image processing and computer vision (Kim and Cho, 2018), while the process of detecting cracks is governed by an onboard microcontroller, MyRio.

The ZigBee (Xbee) wireless technology protocol is used to communicate between the PC and the microcontroller. The UGV actuators and batteries are connected to the microcontroller, MyRio. Using the 4K camera attached to the drone, it will search for cracks. Image processing will be carried out once a crack has been detected. This step begins by capturing images from the thermal and laser depth cameras and sending them to the MyRio, which uses computer vision and related image processing techniques to identify the crack shape, type, and other parameters. The results will then be sent to the PC and displayed on the LabVIEW front panel.

Webots simulate the integrated system using a fully programmed drone equipped with all of the necessary sensors to allow drone stabilization and crack visualization via a camera sensor. Fig. 2 simulates the entire design process of the system in a real-world environment.

2.2. Detailed design

2.2.1. UGV assembly model

Fig. 3 depicts the UGV assembly drawings. It demonstrates the precise location of sensing elements as well as the landing platform for drones. This design was implemented to ensure compatibility with a variety of road characteristics.

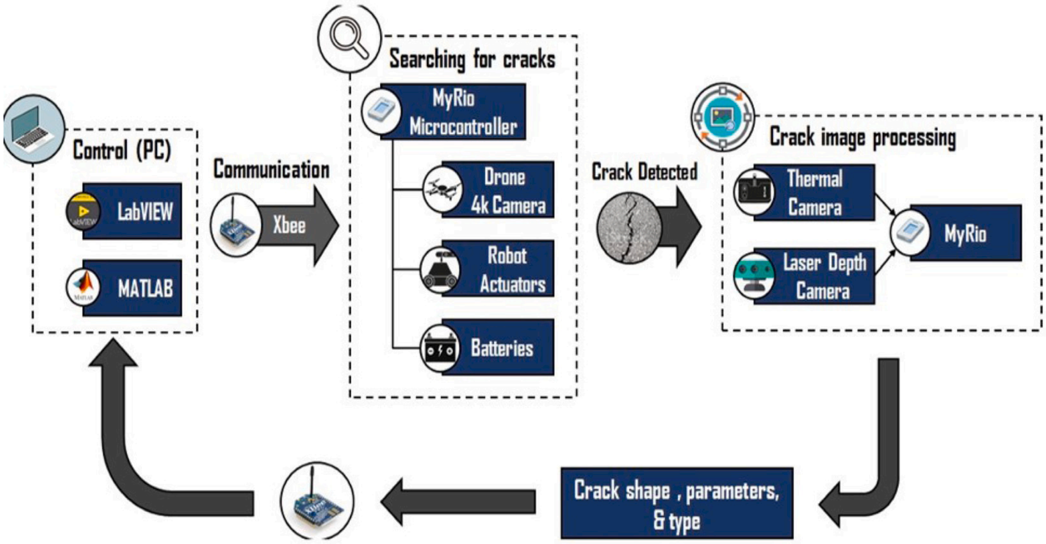

Fig. 1. Overall system architecture.

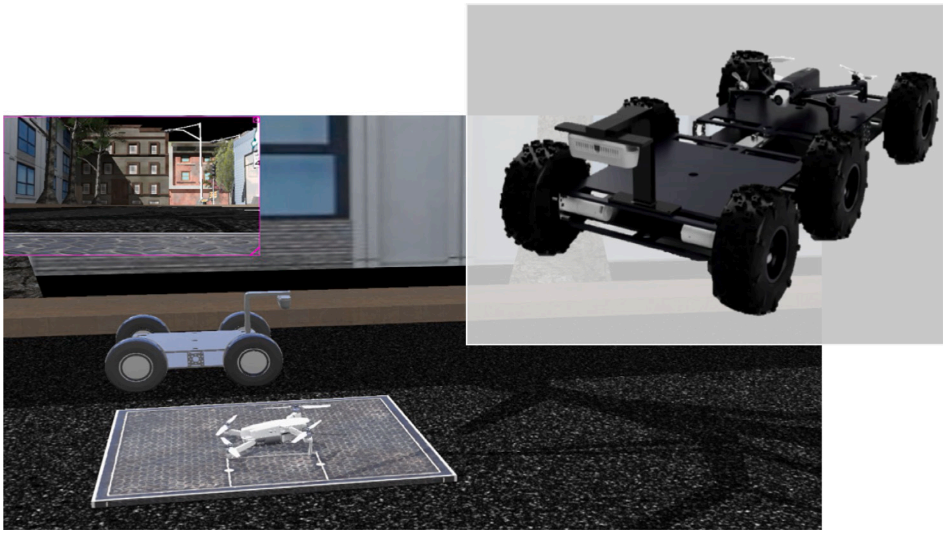

Fig. 2. Visualized UGV and drone integrated system.

2.2.2. System components

myRIO is the primary microcontroller used to control the UGV. In comparison to other microcontrollers, the Field Programmable Gate Array (FPGA) is capable of assisting users in solving problems more quickly and efficiently (Wang et al., 2020). The thermal camera used is the FLIR C3, which is intended to inspect buildings, HVAC systems, and electrical circuits. It has an object temperature range of −10 to 150 °C, the accuracy is ±2 °C, and thermal sensitivity is less than 0.1 °C. Additionally, it features a touchscreen and the ability to share photos via Wi-Fi (LIR, 2017). Additionally, an Intel D415 RealSense depth camera produces a visual image and a 3D depth map. The depth map provides the measured distance from the camera, while the RGB image provides a high-quality visual representation with 1920 × 1080 resolution and 2 MP. The depth map is visualized in the Intel RealSense SDK 2.0 program. All camera setups can be adjusted automatically depending on the maximum and the minimum depth measured in the image. We aligned the field of view experimentally to ensure the camera's correct placement. As such, the depth camera sensors are located in the front of the robot on an L shape camera holder so that the camera view direction is perpendicular to the road and to ensure the depth distance is correctly measured. The height of the camera is at 50 cm with a capture frame rate of 30 frames per second. However, the thermal camera is impeded in the Drone camera, and its view can be controlled. The implemented program run by Parrot allows users/developers to access the drone's live feed and stream to any Linux-based device; in our case, the Raspberry Pi 4 is used (Zalud, 2016). The live feed is inputted to the proposed image processing pipeline, which is then used to examine defects

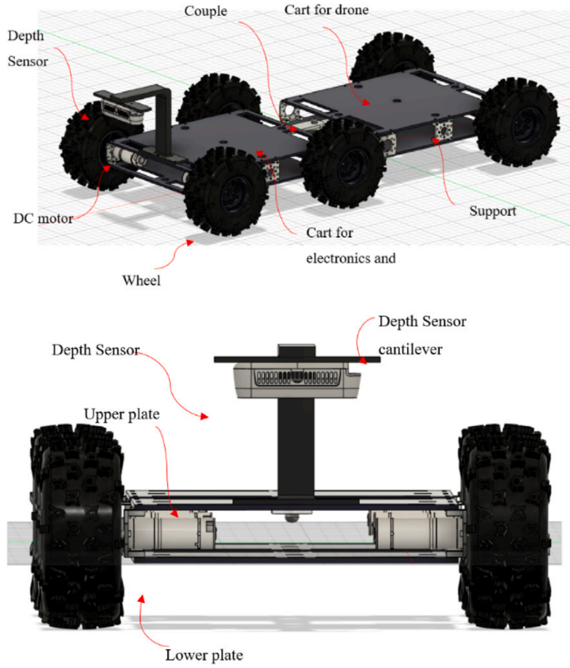

Fig. 3. UGV assembly 3D model.

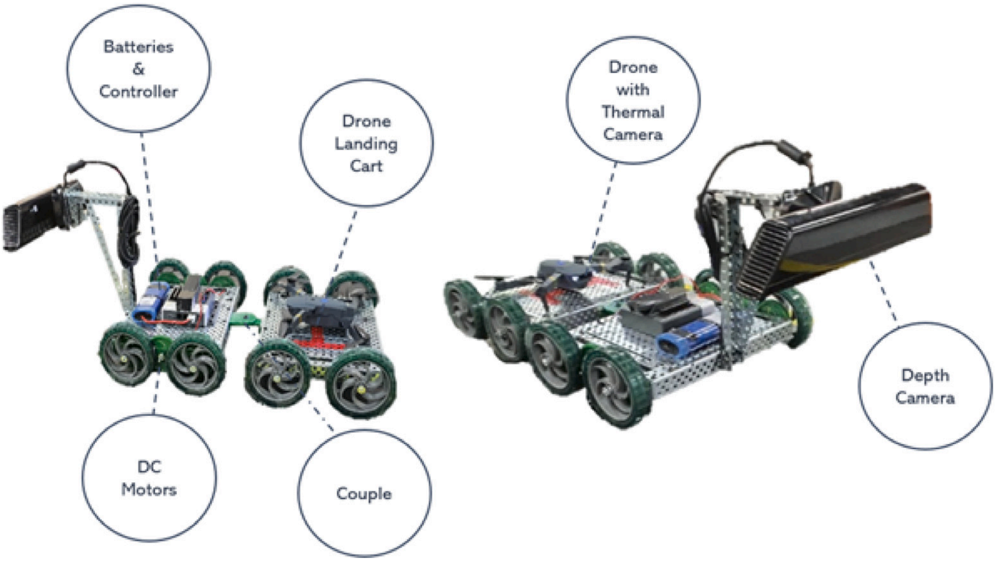

Fig. 4. UGV-Drone prototype assembly.

in the road being inspected. ZigBee can transfer streamed data to a remote workstation for further analysis of the feed stream. The initial prototype of the UGV-drone system for indoor testing is depicted in Fig. 4.

As shown in Fig. 4, the drone utilized has a quadcopter configuration, which enables simple and easy control of the drone and more precise turns through the use of simple electronics (Kim et al., 2018). The proposed UGV method consists of two bodies. The primary body comprises microcontrollers, motors, and sensors. The second body is an extension of the first body that serves as a drone station. Weak magnets secure the drone and enable wireless charging. Using manual detachment, the second cart can be detached from the first cart to serve as a charging station for both devices or in the event of an emergency or maintenance. This design allows the UGV to move freely in all directions while overcoming ground debris in the working environment.

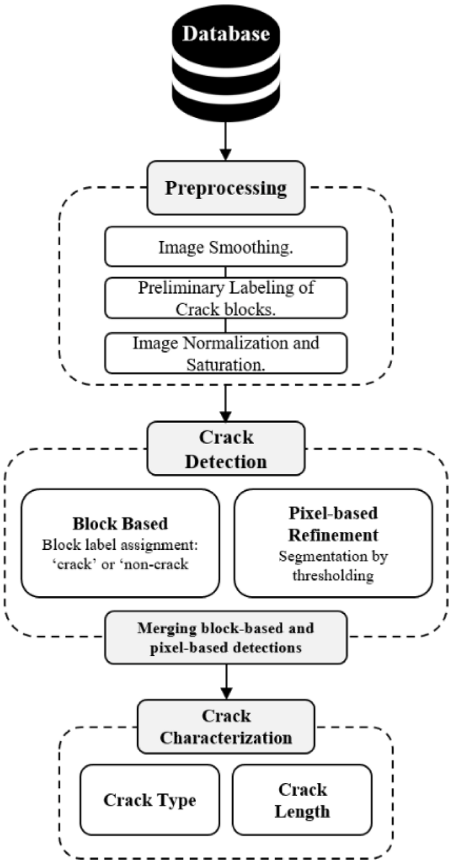

Fig. 5. Crack detection image processing system architecture.

We built the prototype using light aluminum due to its strength and corrosion resistance properties. Moreover, rubber wheels are used to decrease vibrations. The 4 DC motors operate the four wheels, each with 12 V, 0.14 A, and a maximum speed of 3500RPM. These motors ensure a maximum speed of 1.5 m/s, and the operation speed will be one m/s.

2.3. System implementation

2.3.1. Crack detection using image analysis

The crack database was created by crowd-sourcing the activity to citizen scientists. We create an online form which captures image of a crack and the location where the crack was found. The citizen scientists lived all over city of Abu Dhabi in the United Arab Emirates. Their submission was then evaluated by experts to ensure a balanced dataset. Experts also manually segmented the cracks and generated ground truth masks using Photoshop. The quality of the ground truth images was evaluated and confirmed before it was used to assess the performance of our newly proposed segmentation and that of the CrackIT as a baseline performance.

The crack detection is performed using image processing and CrackIT toolboxes in MATLAB. Parameters related to the tuned threshold value to segment the images, the constant that controls the diffusion speed for image smoothing, and saturation intensity were modified in the CrackIT code to become suitable for the visual image colors. The finalized adapted software includes measuring the crack length to detect the crack and identify its type and length. The implemented image processing pipeline is depicted in Fig. 5. It begins with creating a cracks database, pre-processing steps, crack detection using block-based and pixel-based methods, and finally, crack characteristics determination.

The pre-processing stage is proposed for modulation in the CrackIT system (Oliveira and Correia, 2014; Yeum and Dyke, 2015); the steps comprise: (1) image smoothing, which focuses on reducing the road surface background and texture randomness without relapsing the crack details, (2) labeling crack blocks containing relevant cracks and their corresponding locations, thus avoiding mislaying crack information in the normalization and saturation steps, and (3) image normalization and saturation; this step focuses on making the intensities equal to image blocks of previous images with no cracks; this decreases the non-uniform image illumination of the background and reduces the specular reflection impact induced by refined pavement surface blocks. These image processing techniques, including smoothing, normalization, and contrast enhancement, deal with lens distortion and any variation in camera acquisition.

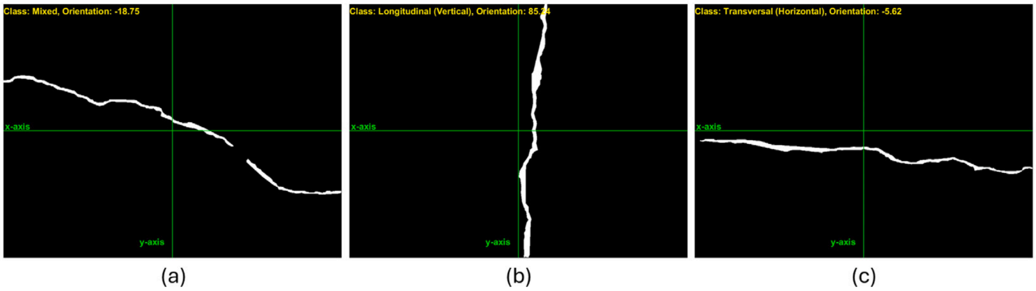

Fig. 6. Determining the orientation of the segmented cracks.

The crack detection stage employs two distinct algorithms: block-based and pixel-based. The block-based method (Abdellatif et al., 2021) uses a pattern identification algorithm that classifies non-overlapping blocks as 'crack' or 'non-crack.' The pixel-based process segments the pre-processed images based on a tuned intensity threshold. Then, the potential cracks are determined by grouping the crack pixels using a connected components algorithm. We use binary feature extraction techniques to analyze the crack blobs and calculate the height and width after correcting for orientation.

The image is converted to grayscale, and the crack is initially identified based on the intensity of the image segments. The histogram is computed using image intensities. This histogram depicts the method used to detect the crack in the grayscale image by using a tuned intensities threshold. The image segmentation process employs thresholding to determine the location of crack boundaries.

We also design and implement a real-time segmentation algorithm to further improve the crack detection segmentation describes in Algorithm 1.

Algorithm 1 Proposed real-time segmentation method

Step 1: Saturate the bottom 1% and the top 1% of all pixel values to increase contrast
Step 2: Use a low-sensitivity adaptive threshold calculated from local neighborhood statistics
Step 3: Use binary feature extraction to filter poorly connected blobs out
Step 4: Apply morphological dilation with a 5-pixel disk structuring element
Step 5: Post-process with a blurring and hole-filling filters

The detected cracks are classified into three basic types based on their orientation: longitudinal, transversal, and mixed cracks based on their width measurement. Transversal cracks are the ones appearing horizontally in the captured frame. Longitudinal are the ones appearing vertically, and mixed cracks cannot be determined as either without further assessment, appearing diagonally. The crack width is determined using the ratio of the area of crack segments to the total number of crack pixels associated with the crack frame, as presented in Algorithm 2.

Algorithm 2 Crack characterization

Step 1: Merge block-based and pixel-based detection (binary matrices)
Step 2: Create connected component crack blocks
Step 3: Feature extraction:

1. Standard deviation column
2. Standard deviation row

Step 4: Crack type Detected:

- Longitudinal crack: if the nearest axis is horizontal X-axis (Cracks perpendicular to the pavement's centerline)
- Transversal crack: if the nearest axis is vertical Y-axis (Cracks parallel to the pavement's centerline)
- Mixed crack: if the nearest axis cannot be determined

Step 5: Compute crack skeleton
Step 6: Compute crack reference width

The orientation of the crack in the segmented binary image is determined using the second-order moments of the blob region. The angle θ, represents the counterclockwise angle (in degrees) between the x-axis and the major axis of the crack computed using Eq. (1). Sample of determining the cracks class through its orientation is illustrated in Fig. 6.

$$\theta = \frac{1}{2}\arctan\left(\frac{2\mu_{xy}}{\mu_{xx}-\mu_{yy}}\right) \tag{1}$$

where μ_{xx} and μ_{yy} are the second-order central moments along the x-axis and y-axis, respectively, and μ_{xy} is the mixed second-order central moment.

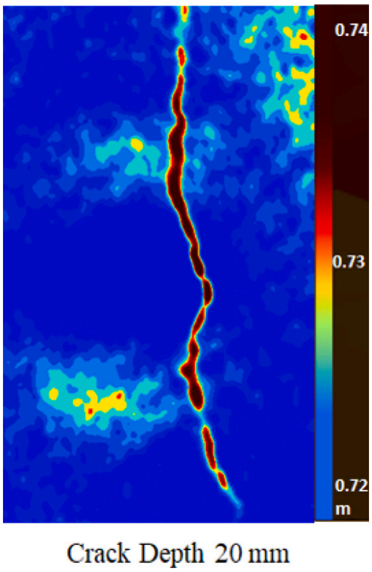

Fig. 7. Heat map of the crack depth captured by the D415 depth camera.

2.3.2. Thermal imaging of crack area

The second method for detecting road cracks is to use a thermal camera to compare the temperature of the crack to that of the surrounding road areas. Through testing, it has been discovered that the crack temperature is higher than the road temperature and that the relative color contrast indicates crack depth and severity. The increase of crack temperature is relative to the depth and width of the crack. The color contrast in the thermal image is used in conjunction with image processing and color recognition to determine the severity of the crack.

The imported thermal image undergoes several image processing steps to extract crack information. Next, the image data is converted to a double RGB color map. Each color output is multiplied by a different threshold to convert the image to grayscale. The results will then be combined and passed through a two-dimensional Finite Impulse Response (FIR) filter. The most significant advantage of this filter is that it operates independently of image parameters such as format and size, which simplifies and clarifies the process.

2.3.3. Depth camera crack analysis

In addition to thermal imaging, a depth camera is incorporated to validate crack detections and provide depth-specific information. This dual-sensor approach aids in distinguishing true cracks from other surface irregularities by using depth data to verify the thermal readings. This validation layer reduces false positives, particularly in cases where non-crack features may exhibit similar thermal characteristics to actual cracks.

The Intel D415 RealSense depth camera calculates the crack depth dimensions via stereo capture. The D415 is equipped with two RGB sensors and an infrared projector. The depth camera D415 employs a powerful image processor with a 28 nm process technology that supports up to 5 MIPI cameras to increase output speed and calculate real-time depth images. The depth camera, with an accuracy of ±2% and a sensitivity of 0.1 °C, measures crack depth within a range of up to 50 cm.

D415 employs an advanced depth algorithm for long-range and very accurate depth perception. In this study, a depth camera is used to scan various cracks of varying shapes to calculate the volumetric dimensions of the cracks. Fig. 7 shows a heat map of a 20 mm deep pavement crack captured by the D415 depth camera.

2.3.4. Drone and ground vehicle navigation and localization

Light Detection and Ranging (LiDAR) is a remote sensing technology that uses laser pulses to measure distances by calculating the time-of-flight of reflected light. It generates precise 3D spatial data, enabling real-time obstacle detection and avoidance (Zhu et al., 2024; Kim et al., 2022; Gonzalez-Garcia et al., 2022). Our UGV continuously scans its surroundings to detect obstacles and free spaces. The integrated GPS module provides the UGV's current global location. The drone is accompanied by a flight planning system to enable users to locate the waypoints of the drone on the map within a 4 km range. Fig. 8 represents a map showing the flight path of the drone taken from its flight planning system.

The drone-based inspection system captures high-resolution imagery of the pavement surface, which it compiles into a detailed mosaic map of the surveyed area. This mapping capability enables efficient identification of locations requiring further inspection for pavement cracks. Utilizing an object detection algorithm based on a CNN model, the system identifies areas of interest with high precision. The drone maintains an altitude of 10 meters to optimize detection accuracy, with the camera oriented at an approximately

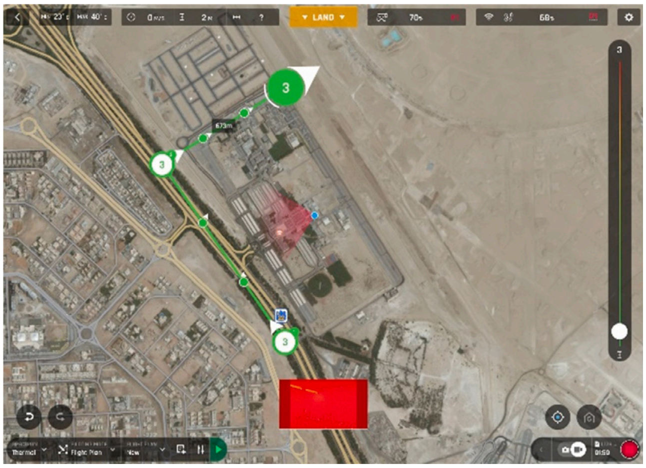

Fig. 8. Flight path of the drone.

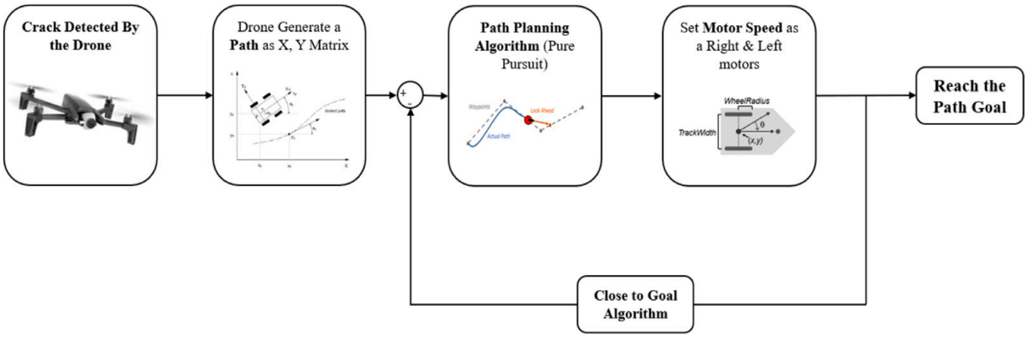

Fig. 9. Path planning block diagram.

95-degree field of view to ensure a comprehensive visual capture of the pavement surface. The detected areas are mapped to real-world coordinates, with latitude and longitude data transmitted to Firebase cloud, as proposed in Ghazal et al. (2020), where it is subsequently accessed by the UGV. The UGV autonomously navigates to these designated coordinates for closer inspection, equipped with thermal and depth cameras aligned parallel to the pavement surface.

The CNN model used for the cracks detection from the drone imagery is YOLOv8s (Jocher et al., 2023) trained on the UAV-PDD2023 dataset (Yan and Zhang, 2023). The dataset consisted of UAV imagery of pavement cracks labeled with multiple classes for object detection tasks, including longitudinal, transverse, alligator, and oblique cracks, repair, and potholes classes. We split the dataset for training and testing at 70% and 30%, respectively, resulting in a mean Average Precision (mAP) of 98.9% and an accuracy of 95.0%.

2.3.5. UGV motion planning and control

MATLAB Simscape multibody simulates UGV motion guided by drone feedback to find cracks. The procedure for path planning is illustrated in Fig. 9.

The UGV is programmed to receive coordinates from the drone after detecting a crack location. The generated path is fed into the UGV path planning algorithm as a reference input. The pure pursuit, Algorithm 3, is used to determine the linear and angular velocities of the robot. The UGV's two velocities are used to calculate the speed of each wheel. The control loop ensures that the UGV tracks and follows the cracks that the overseeing drone has identified.

The Simulink/MATLAB model that integrates motion planning and control procedure for the UGV-guided motion by drone supervisory feedback is shown in Fig. 10.

The Reference Path block is the reference point defined as a waypoint, and it is used as input for the subsequent step, which is the Convert path to motor motion algorithm shown in Fig. 11. This algorithm converts the waypoints to linear and angular velocities using the pure pursuit algorithm, the main block responsible for the path function. The two velocities used as an input to the robot bicycle block are converted into Vx, Vy, and theta. However, the linear and angular velocity will be used as input for the wheel speed function to convert both velocities to left and right velocities for the left and right robot motors, respectively, as a revolute joint. Furthermore, the Close-to-goal block works as a sensor to monitor the robot and ensure it does not deviate from the input path direction.

Algorithm 3 Pure pursuit

Step 1: Identify the last position of the UGV (x, y, θ)
Step 2: Determine the following targeted location
while the targeted location is not reached **do**
Compute the location on the path nearest to the UGV
Compute a specific look-ahead route
Find the targeted location by moving a distance up the route from the location.
end while
Step 3: Convert targeted location to UGV coordinates
Step 4: Compute desired orientation of the UGV
Step 5: Move UGV towards the targeted location with the desired orientation
Step 6: Obtain a new location and go to the next targeted location

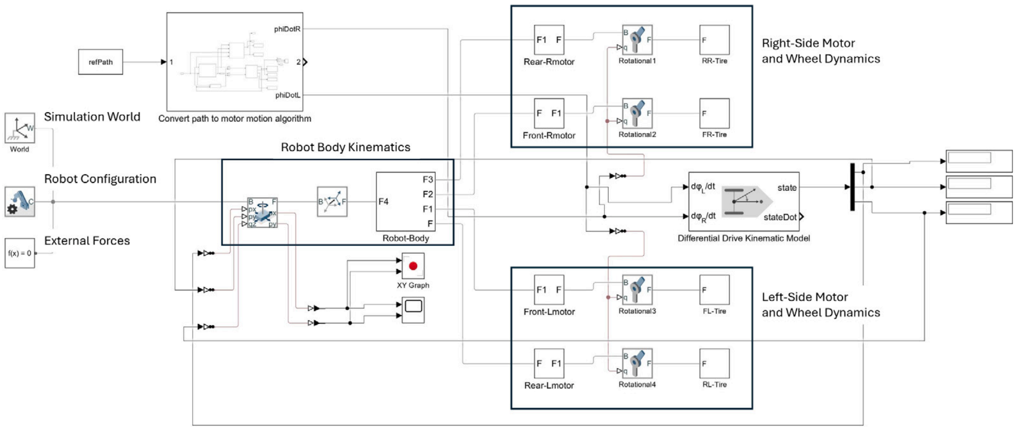

Fig. 10. The Simulink/MATLAB model for the integrated UGV guided motion. We start by setting up the simulation environment parameters (Simulation World, Robot Configuration, and External Forces block), then we monitor the position and orientation of the robot in the environment (Robot Body Kinematics block), then we control the robot's left and right wheels through the right and left sided motors and wheels dynamics blocks, and the Convert path to motor motion algorithm block which outputs the angular velocities of the robot's motors to follow a path starting from the refPath as the entry point. The control is done through a differential drive kinematic model which takes the angular velocities of the right and left wheels and computes the robot's state and velocity to determine the motion trajectory.

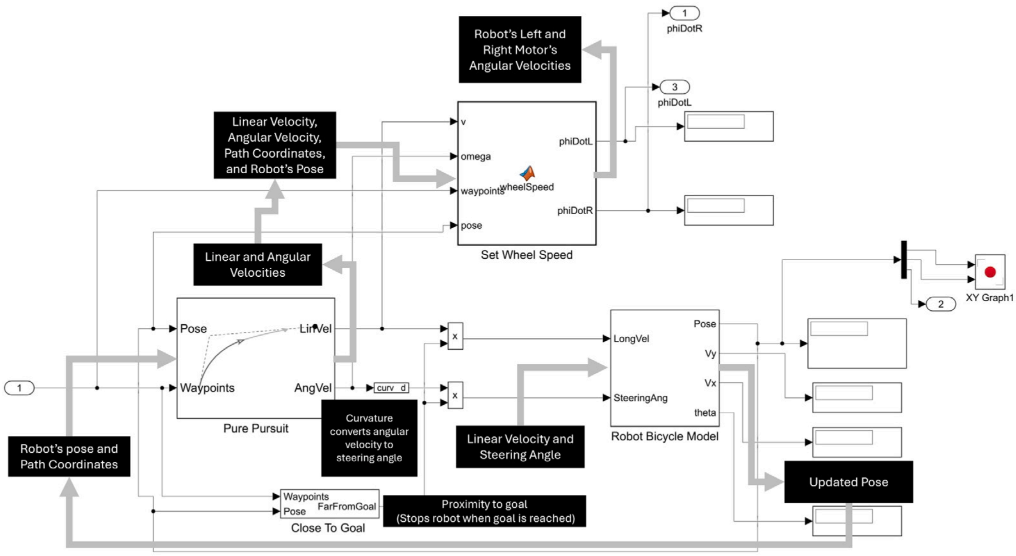

Fig. 11. Convert path to motor motion algorithm block.

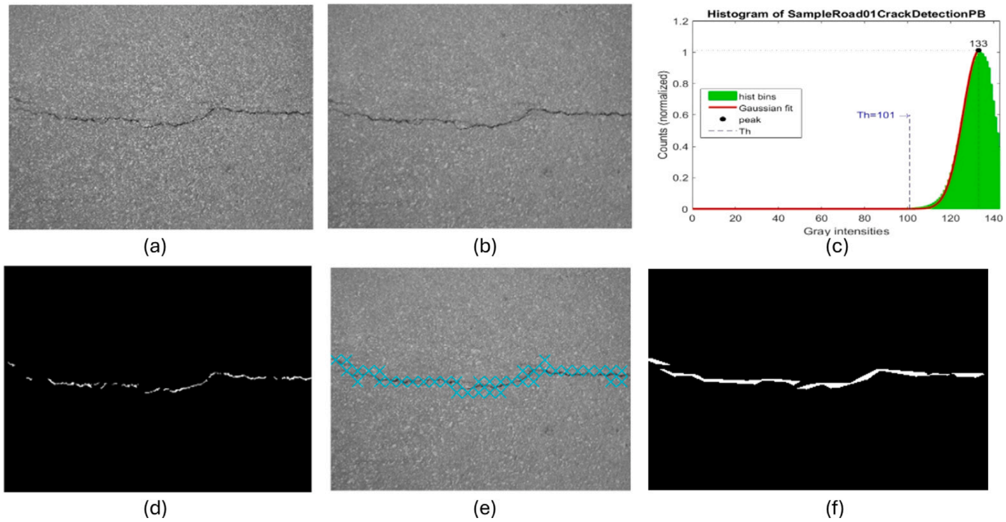

Fig. 12. Crack detection process (a) original crack image, (b) image smoothing, (c) counts vs. grey intensities chart (d) image segmentation result, (e) crack type (transversal crack) after applying morphological dilation to the segmented mask, and (f) the ground truth of the image.

3. Results and discussion

3.1. Crack detection results and analysis

Fig. 12 demonstrates an example of detecting a transversal crack with the use of a MATLAB computing server. The original detected crack image first undergoes smoothing to reduce the road surface background and texture randomness, as shown in Fig. 12(b). Using image intensities, the histogram is computed as shown in Fig. 12(c). This histogram depicts the method for detecting the crack in the grayscale image using a tuned intensities threshold. The image segmentation uses thresholding to locate crack boundaries. The crack after it undergoes threshold-based segmentation followed by morphological dilation is shown in Fig. 12(d) to differentiate between the crack pixels and the background. Finally, the crack is obtained and characterized in Fig. 12(e).

We test our end-to-end system around Abu Dhabi University in Abu Dhabi City, United Arab Emirates, in particular road areas and document the results in Fig. 13. We present multiple RGB visual longitudinal crack areas with their corresponding thermal and depth images in Fig. 13 . It can be noticed from the thermal images that the cracks develop different temperature patterns based on their exposure to the sun. The thermal camera always showed a difference between the temperature of the crack and the ground especially during sunny times and at night. The cracks showed higher temperatures varying from 38.3–38.7° compared to the minimum temperature of the pavement of around 35° on a sunny summer day. The increase in crack temperature was noticed to be relative to the depth and width of the crack. The imported thermal image undergoes several image processing steps to extract crack information demonstrated as the Segmented Pavement Crack in Fig. 13. The depth images reflect the crack depth color profile using the Intel D415 RealSense depth camera. Fig. 13 results show different color maps to differentiate between the cracks and surroundings based on depth dimensions. The accuracy of the depth camera as reported by the manufacturer is 2% and the sensitivity is less than 0.1 °C (Intel.com., 2019). Currently, our system reports only the maximum depth of the detected crack. However, by implementing image registration between the depth image and the segmented pavement crack, the system can accurately detect the entire crack within the depth image and compute the average depth along the entire length of the crack, providing a more comprehensive analysis.

The crack, shown in Fig. 13 were detected by the drone and checked by the UGV in the locations depicted in Fig. 14. This map represents Abu Dhabi University and the area surrounding it where the testing took place.

The traffic is typically average in these areas, and we chose the time of the day that will come with the lowest traffic possible to conduct our tests. Such traffic and timing considerations are typical for any crack detection system. For instance, regular inspection processes require streets to be blocked, reducing the traffic to a standstill, which takes significantly longer than we suggest.

More samples of the images as they undergo crack detection algorithm are shown in Table 2. The cracks are classified into their 3 main types, while the crack length is calculated using pixel measurements, which are then converted to millimeters. The image's dimensions in pixels and the crack length will be visible. We calibrated the cameras and obtained their intrinsic and extrinsic parameters. Given the known pixel size, we obtain the crack length in mm. For instance, when the length of the crack is 2846 pixels, the crack is found to be 753.0 mm after conversion. With camera calibration and the intrinsic and extrinsic parameters known, variations in crack length resulting from flying in the same area are controlled and corrected.

The real-world application of this system is typically by governments with these autonomous robots driving around surveying streets and reporting on their health and locations of the cracks. The possible limitations would be integrating the system within

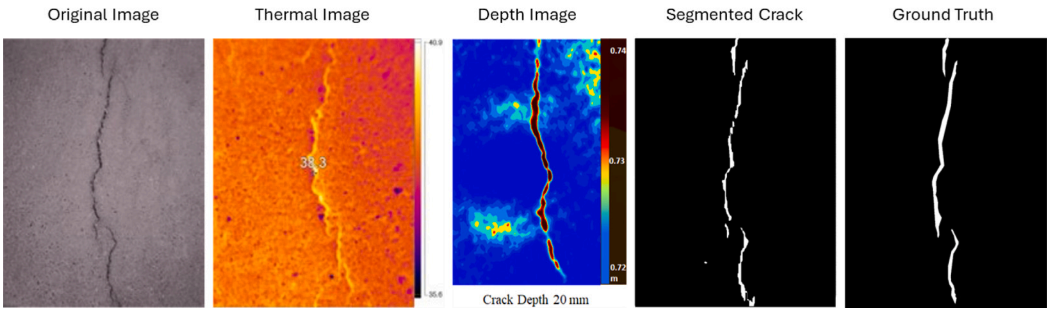

Fig. 13. Sample of a detected crack in RGB scale, thermal, depth and segmented crack image vs. the ground truth.

Fig. 14. Abu Dhabi University location as shown on Google Maps. Latitude and Longitude coordinates for the exact location of the sample crack presented in Fig. 13.

a busy environment in the roads to stop the streets and do the survey, but the robot can be used at times while the street is not busy. The scanning system can be scheduled based on the traffic for the highways and busy streets. On the other hand, there are cities filled with internal roads that are much less traveled and in terrible conditions in many places worldwide. In this case, there are few cars, and the traffic is less, so the system can run well at an off-peak hour and get an entire map for the location of cracks which can help in terms of decisions on road maintenance and municipality decisions, etc.

Assuming a 1 km road with three lanes and drone's speed of 8 km/h, the drone can perform the full scan of the road in 450 s. If the drone detects three cracks in this 1 km road, with the distance between them being 0.7 km, the UGV will move in a path for 0.7 km to scan the cracks at 4 km/h in 630 s. In total, the whole process will take around 1080 s. By comparing our solution with another UGV solution, such as the one presented in Ramalingam et al. (2021), our drone-UGV solution takes less time. For instance, the speed of the UGV in Ramalingam et al. (2021) is 3 km/h, and for it to perform the full scan, it will cover an overall distance of 3 km given the same 3-lanes road. Thus, it will take around 2160 s to scan the 1 km road. As such, our proposed drone-UGV will reduce the road inspection time and road closure by almost 50%.

3.2. Performance evaluation

We evaluate the performance of our proposed classification algorithms using (1) Recall (re), which accounts for false negatives, (2) Precision (pr), which accounts for the presence of false positives, (3) F-measure (Fm) metrics, (4) Error-rate ($e - r_G$), and (5) Crack error-rate ($e - r_{Cr}$) for the intended application. Images acquired during a visual pavement surface inspection are used to evaluate the performance of the proposed crack detection and characterization algorithms, together with severity level assignment methods. The evaluation database comprises 56 gray-level images with ground truth data, where no cracks appear in eight of these

Table 2
Samples of analysis road images for crack type and total length detection. Transversal cracks appear horizontally, longitudinal cracks appear vertically, and mixed cracks cannot be determined as either without further assessment, appearing diagonally.

Original Image	Detected Pavement Crack	Ground Truth	Detected Pavement Crack Type	Crack Length (mm)
	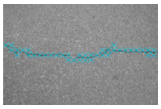		Transversal	548.7458
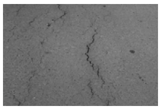	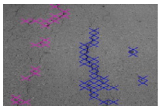		Longitudinal	534.9875
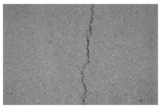	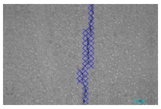		Longitudinal	622.0354
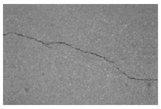	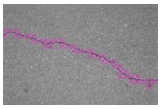		Mixed	729.9854
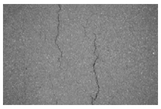	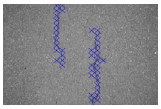		Longitudinal	548.2167

Table 3
Crack detection results for test set images.

Strategy	$e-r_G$	$e-r_{Cr}$	re_{Cr}	pr_{Cr}	Fm_{Cr}
H. Clust.	1.1%	22.5%	77.5%	**99.4**%	86.0%
k-means	0.7%	12.2%	87.8%	97.6%	91.9%
Mixt. Gauss	**0.6**%	4.5%	95.5%	92.2%	**93.5**%
OC-Gauss	0.8%	13.3%	86.7%	97.1%	91.0%
OC-Parzen	1.2%	5.0%	95.0%	84.5%	88.8%

images. The global metrics, error-rate ($e-r_G$) and crack error-rate ($e-r_{Cr}$), can be calculated using Eqs. (2) and (3).

$$e-r_G = \frac{FP+FN}{TP+TN+FP+FN} \tag{2}$$

$$e-r_{Cr} = \frac{FN}{TP+FN} \tag{3}$$

where TP is the True Positives, TN is the True Negatives, FP is the False Positives, and FN is the False Negatives. The positives are the class of blocks with cracks. The negatives are the class of blocks with no cracks. In our application, precision is the difference rate between the number of properly-identified crack blocks and the total number of blocks recognized as cracks. At the same time, recall is the difference rate between the number of correctly detected crack blocks and the number of crack blocks in the ground truth. Table 3 shows a significant performance improvement when using the crack detecting module.

Five unsupervised crack detection techniques are compared, with the one based on a mixture of two Gaussian models attaining the highest overall performance in terms of Fm (93.5%), the lowest global error rate (0.6%), and the second-best recall performance (95.5%).

Unsupervised learning is preferred in this study due to the anomalous nature of crack regions within the idle dataset of pavement structures. In contrast, supervised learning faces challenges related to data quality, as cracks exhibit significant variation in their structure, making it difficult to maintain consistent labeling. This variability reduces the adaptability of supervised systems, whereas unsupervised methods can effectively identify anomalies and patterns without relying on labeled data, ensuring greater flexibility in detecting diverse crack formations.

Table 4
Summary of the data captured parameters.

Parameter	Information
Image resolution	4k (1920 × 1080 pixels)
Physical scaling	0.568 mm/pixel
Image format	JPEG
Lighting conditions	Daylight
Environmental conditions	Clear weather

Gaussian smoothing eliminates many non-crack or non-defect blobs that come from segmentation errors. Also, blob analysis and region of interest filtering eliminate additional errors. For our use case, all road defects, even if they do not conform to the definition of a road crack, are of interest since they play into the local authority's decision to maintain the road according to them.

Hierarchical clustering (H. Clust) (Suzuki, 2023) is a method that builds a nested hierarchy of clusters either by successively merging smaller clusters in a bottom-up fashion (agglomerative) or by dividing larger clusters in a top-down approach (divisive). The resulting dendrogram provides insights into the structure of the data, allowing for flexible cluster determination at different levels of granularity. In contrast, k-means clustering (Saifullah, 2020) is a partition-based method that divides the data into k predefined clusters by iteratively minimizing the within-cluster variance. The algorithm alternates between assigning data points to the nearest cluster center and updating the cluster centers to the mean of assigned points, offering a computationally efficient solution for clustering tasks. A Mixture of Gaussians (Mixt. Gauss) (Riaz et al., 2020), or Gaussian Mixture Model (GMM), represents a probabilistic model that assumes data is generated from a combination of several Gaussian distributions, allowing for the modeling of more complex cluster shapes and soft assignments of data points to multiple clusters based on probability.

In the context of outlier detection, the One-Class Gaussian (OC-Gauss) (Chen et al., 2022) model fits a single Gaussian distribution to the training data and identifies points deviating significantly from this distribution as anomalies. The One-Class Parzen (OC-Parzen) (Cao et al., 2021) method relies on Parzen window estimation to approximate the probability density function of the data. It is often applied in anomaly detection by identifying points that lie in regions of low density, thereby classifying them as outliers. This non-parametric method provides flexibility in estimating complex distributions without assuming a specific parametric form.

3.3. Crack detection performance assessment

We compare our proposed segmentation algorithm to the well-known CrackIT system as a baseline in terms of accuracy, recall, and visual segmentation output.

When tested on our 50 crack images, samples of the data are shown in Fig. 15 and a summary of the details of the data is listed in Table 4, our final accuracy is 99% and recall is 84%, which means that 84% of the true crack pixels were correctly segmented as per the formula in (4) where TP is the true positive pixels and FN is the True Negative pixels. The discrepancy between accuracy and recall is expected due to the huge number of non-crack pixels compared to the crack ones. The accuracy of CrackIT was 98%, but the recall was significantly poorer. With the crack detection method having a recall of 84%, it may miss small newly forming cracks. In fact, crack edges are also sometimes very difficult to label, even for human experts. Nevertheless, precision is less important than recall for the prospective users of the proposed system.

$$recall = \frac{TP}{TP + FN} \tag{4}$$

The visual segmentation results for both CrackIT and our proposed segmentation algorithm are demonstrated in Fig. 16. The black and white pixels are correctly classified, TN and TP respectively, compared to the ground truth. On the other hand, the red and green pixels are false positives and false negatives respectively. It can be observed from the results that CrackIT suffers from a high number of falsely classified pixels compared to our approach.

By designing a better performing crack detection method, we increase the contributions in the paper, where we have succeeded in doing so significantly outperforming CrackIT as a baseline performance in both accuracy and recall to cracks evident by the reported performance metrics. Precision itself is less important to us than recall as we care more about detecting all cracks than the boundaries of each crack. Experts consulted from the municipality decided that not missing cracks (recall) is more important than precisely detecting the crack edges in our application.

We also compare the proposed system as an overall system with existing systems in Table 5 using several criteria including mobility, guidance, defect detection, speed, limitations, accuracy, and recall.

3.4. UGV motion planning and control

The procedure detailed in Section 2.3.5 is tested for different paths in Fig. 17, where the x-axis represents the displacement of the robot in the x-direction in meters, and the y-axis indicates the displacement in the y-direction in meters as the UGV follows the planned paths. The UGV was able to follow the desired path to the crack location based on the reference path detected by the drone.

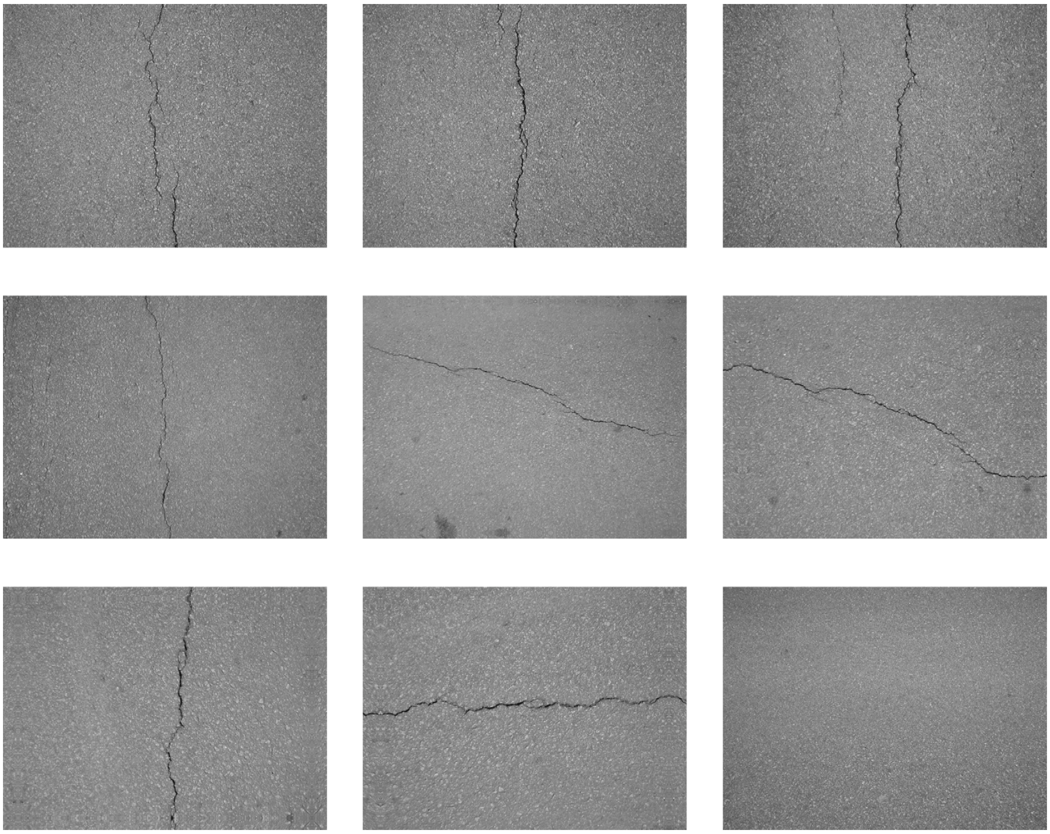

Fig. 15. Samples of the crack images collected for testing.

Table 5
A comparison between our proposed system with existing mobile systems based on mobility, defect detection, speed, limitations, guidance, and accuracy.

	Proposed method	Method 2 (Lim et al., 2014)	Method 3 (Ramalingam et al., 2021)	Method 4 (Feng et al., 2020)
Mobility	High mobility, all terrain	Low mobility, day light conditions only	Low mobility, day light conditions only	High mobility, day light conditions only
Defect Detection	Segmentation-based	Laplacian of Gaussian	Segmentation-based	Segmentation-based
Speed	1.1 m/s	0.1 m/s	0.1 m/s	Driving speed
Limitations	Low traffic times	Limited visual capability and sensing range	Inspection limited to the crack detection, which cannot differentiate between pothole, bumps, etc.	Limited visual capability
Guidance	UAV support	No guidance	No guidance	No guidance
Accuracy	99%	–	95%	87%
Recall	84%	–	–	79.5%

We evaluate the path following the algorithm using the Root Mean Square Error (RMSE) calculated using Eq. (5). We test the algorithm on ten different paths and compare the actual coordinates of the robot to the planned ones to quantitatively evaluate the robot's deviation from the planned path.

$$RMSE = \sqrt{\frac{\sum_{i=1}^{N}\left((x_i - x_i^*)^2 + (y_i - y_i^*)^2\right)}{N}} \tag{5}$$

where N is the total number of data points, (x_i, y_i) are the actual coordinates of the robot's path at point i, and (x_i^*, y_i^*) are the planned coordinates of the robot's path at point i (see Table 6).

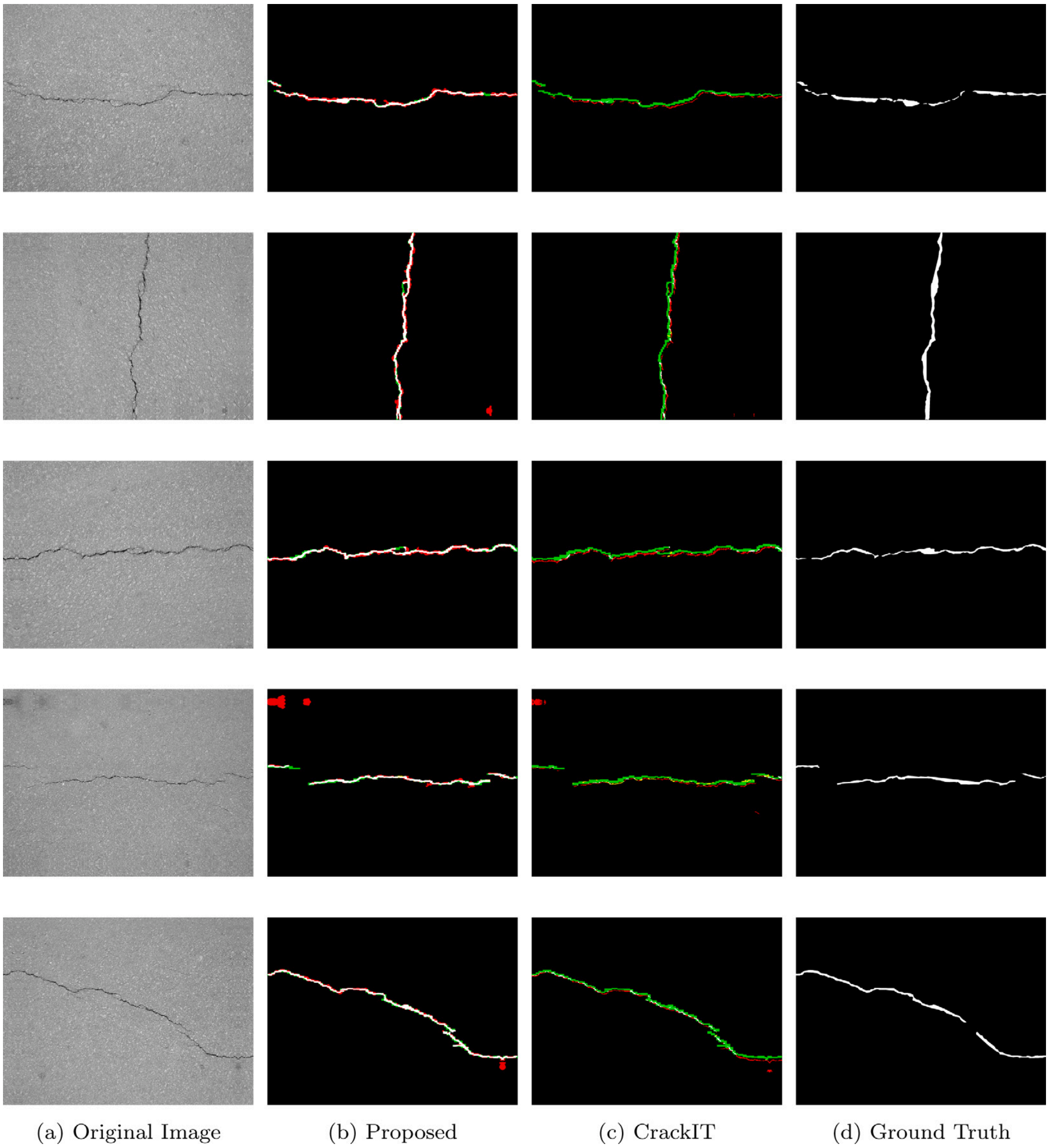

Fig. 16. Black and white pixels are correctly classified compared to the ground truth. Red and green pixels are false positives and false negatives errors.

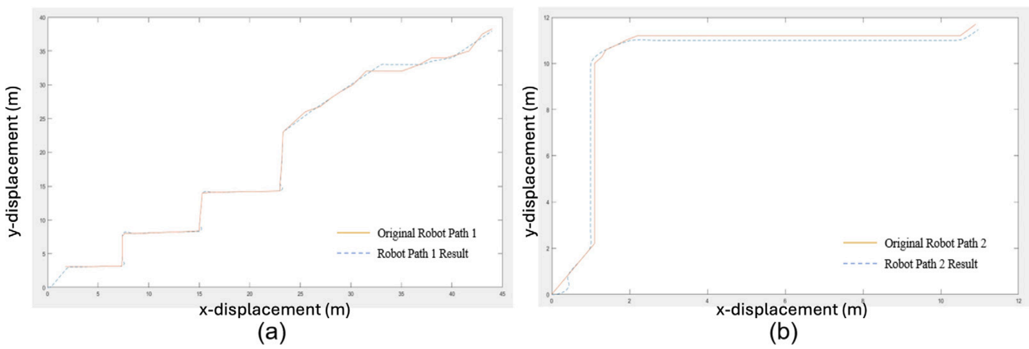

Fig. 17. Planned paths (yellow) and robots paths (blue) comparison where the y and x axes are the displacement in y and x directions in m.

Table 6
Evaluation of the path following algorithm.

Path	RMSE (m)
Path 1	0.087
Path 2	0.145
Path 3	0.123
Path 4	0.110
Path 5	0.066
Path 6	0.066
Path 7	0.056
Path 8	0.137
Path 9	0.110
Path 10	0.121
Average	**0.102**

The aforementioned achieved results can be employed in a vision-based accurate crack identification of pavement and concrete structures using deep learning approaches (Islam and Kim, 2019; Adam and S, 2021; Kim et al., 2020; Saleem and Gutierrez, 2021). The crack will be detected and analyzed to determine the maintenance requirements by fusing and integrating these methods. The initial scan of road images with a drone camera saves time searching for potential pavement crack candidates. The drone sends the location of that potential candidate to the UGV robot, which uses two other inspection methods, thermal imaging, and a laser depth camera, to thoroughly examine the regions of interest. This enables decision-makers to create a road map outlining areas of pavement defects and assigning priority indicators for the maintenance of these defects. Future work could include linking this system to the GIS (Geographic Information Systems) system, which would benefit multiple authorities concerned with road and bridge conditions.

The UAV, flying at an altitude of 10 meters and a field of view of 95 degrees, provides a range of crack detection of approximately 21 m. The UGV has the camera positioned at a height of 50 cm and oriented vertically downward, covering a significantly smaller range of around 1 meter under the same field of view. Thus, using the UAV for crack detection, as its elevated position enables it to scan a broader area with each frame. An autonomous UGV inspecting the pavement would require more time and energy due to its limited field of view in the same area. Therefore, the UAV-UGV combination enhances efficiency and ensures thorough coverage, leveraging the UAV's range to guide the UGV to precise locations for detailed inspection.

4. Limitations and future work

The current robot used for pavement crack detection lacks a suspension system. Without proper suspension, the robot is more susceptible to vibrations from uneven road surfaces, which can significantly affect the stability of the onboard camera and the quality of the captured images. These vibrations may introduce motion blur or distortions, reducing the accuracy of crack detection algorithms. Future work could involve integrating a suspension system or implementing image stabilization techniques to mitigate these effects, enhancing the robot's ability to capture high-quality images on various pavement surfaces.

There are various types of pavement cracks, including transversal, longitudinal, patching, pothole, and alligator cracks, that represent challenges in road maintenance and require precise identification for remediation. As part of future enhancements to our proposed system, we aim to expand the data collection process to include comprehensive datasets that encompass all these crack types. This will enable our classifier to accurately identify and distinguish between each type.

The current system relies on a tuned thresholding approach for segmentation, which was calibrated under specific temperature conditions present in the UAE during testing. This static thresholding may limit the system's accuracy in environments with fluctuating temperature levels, where variations could impact pavement surface texture and appearance, potentially leading to inconsistent detection outcomes. To address this, future work should consider temperature variation effects on segmentation performance, potentially integrating adaptive techniques to accommodate environmental changes. Additionally, advanced segmentation models, such as Segment Anything (Kirillov et al., 2023), could be assessed for their effectiveness in improving segmentation accuracy across diverse environmental conditions. Further evaluation of these methods under varying temperature and lighting conditions could provide insights into enhancing the model's robustness and expanding its applicability to broader geographic settings.

5. Conclusions

This research proposes and implements an advanced coordinated mobile robots sensing system that combines an unmanned ground vehicle (UGV) and a drone to detect pavement defects for structural health monitoring applications. The system is intended to be efficient, practical, durable, portable, and affordable. Our proposed tailored image processing pipeline improves the performance of CrackIT significantly in accuracy and more importantly recall. It also outperforms existing state-of-the-art solutions with its high mobility, speed, crack detection guidance mechanism, accuracy, and recall. The proposed crack detection system is capable of high-precision tasks and can be integrated into smart city applications. The pavement crack parameters were extracted using image processing techniques based on thermal and depth cameras. The thermal camera was able to identify cracks and reveal the crack characteristics and length. The cracks had higher temperatures ranging from 38.3–38.7° relative to the pavement's temperature of roughly 35°. The cracks were successfully classified into three major classes (transversal, longitudinal, and mixed), and the crack length was determined using pixel measurements that were then converted to millimeters. The depth map displays different color mappings to distinguish between cracks and their surroundings based on depth dimensions. Webots software was used to create a virtual environment that demonstrates how the system will perform in real-world applications. Drone imaging was used simultaneously to determine the potential crack location and control the UGV motion and path following crack location. Using the drone's feedback, the integrated system provided the initial establishment of the cracks. Using a pure pursuit algorithm, the UGV could follow the path generated to reach the potential crack locations. The crack characteristics autonomously detected by our proposed system provide authorities with accurate feedback on the pavement's conditions. Future plans include registering the thermal and depth images using their derivatives to overlay them and create a new hybrid image that can help researchers characterize cracks better.

CRediT authorship contribution statement

Mohammad Alkhedher: Writing – review & editing, Writing – original draft, Validation, Supervision, Software, Resources, Project administration, Methodology, Investigation, Funding acquisition, Formal analysis, Conceptualization. **Abdullah Alsit:** Writing – review & editing, Writing – original draft, Visualization, Validation, Software, Resources, Methodology, Investigation, Formal analysis, Data curation. **Marah Alhalabi:** Writing – review & editing, Writing – original draft, Visualization, Validation, Software, Resources, Methodology, Investigation, Formal analysis, Data curation, Conceptualization. **Sharaf AlKheder:** Writing – review & editing, Writing – original draft, Visualization, Software, Resources, Project administration, Methodology, Investigation, Formal analysis, Conceptualization. **Abdalla Gad:** Writing – review & editing, Writing – original draft, Validation, Software, Methodology, Investigation, Formal analysis, Data curation, Conceptualization. **Mohammed Ghazal:** Writing – review & editing, Writing – original draft, Supervision, Resources, Project administration, Methodology, Investigation, Funding acquisition, Data curation, Conceptualization.

Acknowledgment

ADU authors acknowledges financial support from Abu Dhabi University's Office of Research and Sponsored Programs.

Data availability

Data will be made available on request.

References

Abdellatif, M., Peel, H., Cohn, A., Fuentes, R., 2021. Combining block-based and pixel-based approaches to improve crack detection and localization. Autom. Constr. 122, 103492. http://dx.doi.org/10.1016/j.autcon.2020.103492.

Adam, E.B., S, A., 2021. Construction of accurate crack identification on concrete structure using hybrid deep learning approach. J. Innov. Image Process. 3, 85–99. http://dx.doi.org/10.36548/jiip.2021.2.002.

Aleadelat, W., Wright, C., Ksaibati, K., 2018. Estimation of gravel roads ride quality through an android-based smartphone. Transp. Res. Record: J. Transp. Res. Board 2672, 14–21. http://dx.doi.org/10.1177/0361198118758693.

Aygun, L.E., et al., 2020. Large-area resistive strain sensing sheet for structural health monitoring. Sensors 20 (1386), http://dx.doi.org/10.3390/s20051386.

Cantisani, G., Del Serrone, G., 2020. Procedure for the identification of existing roads alignment from georeferenced points database. Infrastructures 6 (2), http://dx.doi.org/10.3390/infrastructures6010002.

Cao, J., Dai, H., Lei, B., Yin, C., Zeng, H., Kummert, A., 2021. Maximum correntropy criterion-based hierarchical one-class classification. IEEE Trans. Neural Netw. Learn. Syst. 32, 3748–3754. http://dx.doi.org/10.1109/TNNLS.2020.3015356.

Chambon, S., Moliard, J., 2011. Automatic road pavement assessment with image processing: Review and comparison. Int. J. Geophys. 2011, 1–20. http://dx.doi.org/10.1155/2011/989354.

Chen, S., Feng, Z., Xiao, G., Chen, X., Gao, C., Zhao, M., Yu, H., 2024. Pavement crack detection based on the improved swin-unet model. Buildings 14, http://dx.doi.org/10.3390/buildings14051442.

Chen, Y., Tian, Y., Pang, G., Carneiro, G., 2022. Deep one-class classification via interpolated Gaussian descriptor. Proc. AAAI Conf. Artif. Intell. 36, 383–392. http://dx.doi.org/10.1609/aaai.v36i1.19915.

Chen, L., Wang, M., Lin, D., Trsi, S., 2013. Assessing the quality of asphalt concrete pavement at special locations with infrared thermal imager. Adv. Mater. Res. 723, 35–40. http://dx.doi.org/10.4028/www.scientific.net/amr.723.35.

Choi, W., Park, K., 2019. Array type miniaturized ultrasonic sensors to detect urban sinkholes. Measurement 141, 371–379. http://dx.doi.org/10.1016/j.measurement.2019.04.043.

Chun, P., Yamane, T., Tsuzuki, Y., 2021. Automatic detection of cracks in asphalt pavement using deep learning to overcome weaknesses in images and GIS visualization. Appl. Sci. 11 (892), http://dx.doi.org/10.3390/app11030892.

Ciampoli, L.B., Tosti, F., Economou, N., Benedetto, F., 2019. Signal processing of GPR data for road surveys. Geosciences 9 (96), http://dx.doi.org/10.3390/geosciences9020096.

Dong, Q., Wang, S., Chen, X., Jiang, W., Li, R., Gu, X., 2023. Pavement crack detection based on point cloud data and data fusion. Philos. Trans. R. Soc. A 381, http://dx.doi.org/10.1098/rsta.2022.0165.

Dorafshan, S., Thomas, R., Maguire, M., 2019. Benchmarking image processing algorithms for unmanned aerial system-assisted crack detection in concrete structures. Infrastructures 4 (19), http://dx.doi.org/10.3390/infrastructures4020019.

Feng, X., Xiao, L., Li, W., Pei, L., Sun, Z., Ma, Z., Shen, H., Ju, H., 2020. Pavement crack detection and segmentation method based on improved deep learning fusion model. Math. Probl. Eng. 2020.

Garg, S., Misra, S., 2020. Efficiency of NDT techniques to detect voids in grouted post-tensioned concrete ducts. Nondestruct. Test. Eval. 1–22. http://dx.doi.org/10.1080/10589759.2020.1758100.

Ghazal, M., Basmaji, T., Yaghi, M., Alkhedher, M., Mahmoud, M., El-Baz, A.S., 2020. Cloud-based monitoring of thermal anomalies in industrial environments using AI and the internet of robotic things. Sensors 20, http://dx.doi.org/10.3390/s20216348, URL: https://www.mdpi.com/1424-8220/20/21/6348.

Golrokh, A.J., Gu, X., Lu, Y., 2021. Real-time thermal imaging-based system for asphalt pavement surface distress inspection and 3D crack profiling. J. Perform. Constr. Facil. 35, http://dx.doi.org/10.1061/(ASCE)CF.1943-5509.0001557.

Gonzalez-Garcia, A., Collado-Gonzalez, I., Cuan-Urquizo, R., Sotelo, C., Sotelo, D., Castañeda, H., 2022. Path-following and LiDAR-based obstacle avoidance via NMPC for an autonomous surface vehicle. Ocean Eng. 266 (Part 3), 112900. http://dx.doi.org/10.1016/j.oceaneng.2022.112900.

Guo, F., Liu, J., Xie, Q., Yu, H., 2024. A two-stage framework for pixel-level pavement surface crack detection. Eng. Appl. Artif. Intell. 133, http://dx.doi.org/10.1016/j.engappai.2024.108312.

Harikrishnan, P.M., Gopi, V.P., 2017. Vehicle vibration signal processing for road surface monitoring. IEEE Sensors J. 17, 5192–5197. http://dx.doi.org/10.1109/JSEN.2017.2719865.

Intel.com., 2019. Intel RealSense™ camera 400 series (DS5) product family datasheet. URL: https://www.intel.com/.

Islam, M., Kim, J., 2019. Vision-based autonomous crack detection of concrete structures using a fully convolutional encoder–decoder network. Sensors 19 (4251), http://dx.doi.org/10.3390/s19194251.

Jiang, J., Li, P., Wang, J., Chen, H., Zhang, T., 2024. Asphalt pavement crack detection based on infrared thermography and deep learning. Int. J. Pavement Eng. 25, http://dx.doi.org/10.1080/10298436.2023.2295906.

Jocher, G., Chaurasia, A., Qiu, J., 2023. Ultralytics YOLOv8. URL: https://github.com/ultralytics/ultralytics. License: AGPL-3.0.

Kim, B., Cho, S., 2018. Automated vision-based detection of cracks on concrete surfaces using a deep learning technique. Sensors 18 (3452), http://dx.doi.org/10.3390/s18103452.

Kim, I., Jeon, H., Baek, S., Hong, W., Jung, H., 2018. Application of crack identification techniques for an aging concrete bridge inspection using an unmanned aerial vehicle. Sensors 18 (1881), http://dx.doi.org/10.3390/s18061881.

Kim, J., Kim, A., Lee, S., 2020. Artificial neural network-based automated crack detection and analysis for the inspection of concrete structures. Appl. Sci. 10 (8105), http://dx.doi.org/10.3390/app10228105.

Kim, H., Lee, J., Ahn, E., Cho, S., Shin, M., Sim, S., 2017. Concrete crack identification using a UAV incorporating hybrid image processing. Sensors 17 (2052), http://dx.doi.org/10.3390/s17092052.

Kim, J.-S., Lee, D.-H., Kim, D.-W., Park, H., Paik, K.-J., Kim, S., 2022. A numerical and experimental study on the obstacle collision avoidance system using a 2D LiDAR sensor for an autonomous surface vehicle. Ocean Eng. 257, 111508. http://dx.doi.org/10.1016/j.oceaneng.2022.111508.

Kirillov, A., Mintun, E., Ravi, N., Mao, H., Rolland, C., Gustafson, L., Xiao, T., Whitehead, S., Berg, A.C., Lo, W.-Y., Dollár, P., Girshick, R., 2023. Segment anything. URL: https://arxiv.org/abs/2304.02643. arXiv:2304.02643.

Koohmishi, M., Kaewunruen, S., Chang, L., Guo, Y., 2024. Advancing railway track health monitoring: Integrating GPR, InSAR, and machine learning for enhanced asset management. Autom. Constr. 162, 105378. http://dx.doi.org/10.1016/j.autcon.2024.105378.

Lai, W.W.-L., Dérobert, X., Annan, P., 2018. A review of ground-penetrating radar application in civil engineering: A 30-year journey from locating and testing to imaging and diagnosis. NDT E Int. 96, 58–78. http://dx.doi.org/10.1016/j.ndteint.2017.04.002.

Lang, H., Lu, J.J., Lou, Y., Chen, S., 2020. Pavement cracking detection and classification based on 3D image using multiscale clustering model. J. Comput. Civ. Eng. 34, http://dx.doi.org/10.1061/(ASCE)CP.1943-5487.0000910.

Lei, N., Wang, P., Xu, P., Song, G., 2018. New crack detection method for bridge inspection using UAV incorporating image processing. J. Aerosp. Eng. 31, 04018058. http://dx.doi.org/10.1061/(ASCE)AS.1943-5525.0000879.

Li, J., Zhang, Z., Wang, W., 2019. New approach for estimating international roughness index based on the inverse pseudo excitation method. J. Transp. Eng. B 145, 04018059. http://dx.doi.org/10.1061/jpeodx.0000093.

Lim, R.S., La, H.M., Shan, Z., Sheng, W., 2011. Developing a crack inspection UGV for bridge maintenance. In: 2011 IEEE International Conference on Robotics and Automation. pp. 6288–6293. http://dx.doi.org/10.1109/ICRA.2011.5980131.

Lim, R., La, H., Sheng, W., 2014. A robotic crack inspection and mapping system for bridge deck maintenance. IEEE Trans. Autom. Sci. Eng. 11, 367–378.

Lin, Y.-C., Manish, R., Bullock, D., Habib, A., 2021. Comparative analysis of different mobile LiDAR mapping systems for ditch line characterization. Remote. Sens. 13 (2485), http://dx.doi.org/10.3390/rs13132485.

LIR, F., 2017. FLIR launches five new thermal cameras: Third generation FLIR ONEs, FLIR duo thermal/visible drone cameras, and FLIR C3 rugged pro camera. Meas. Control. 50, 22–23. http://dx.doi.org/10.1177/0020294017703849.

Merkle, D., Schmitt, A., Reiterer, A., 2020. Concept of an autonomous mobile robotic system for bridge inspection. In: Remote Sensing Technologies and Applications in Urban Environments V. http://dx.doi.org/10.1117/12.2570633.

Nguyen, T., Lechner, B., Wong, Y., 2019. Response-based methods to measure road surface irregularity: A state-of-the-art review. Eur. Transp. Res. Rev. 11. http://dx.doi.org/10.1186/s12544-019-0380-6.

Nichols, P., McCallum, A., Lucke, T., 2017. Using ground-penetrating radar to locate and categorise tree roots under urban pavements. Urban For. Urban Green. 27, 9–14. http://dx.doi.org/10.1016/j.ufug.2017.06.019.

Oliveira, H., Correia, P.L., 2014. Crackit–an image processing toolbox for crack detection and characterization. In: 2014 IEEE International Conference on Image Processing. ICIP, pp. 798–802. http://dx.doi.org/10.1109/ICIP.2014.7025160.

Pan, Y., et al., 2016. Road pavement condition mapping and assessment using remote sensing data based on MESMA. IOP Conf. : Earth Environ. Sci. 34, 012023. http://dx.doi.org/10.1088/1755-1315/34/1/012023.

Prasanna, P., et al., 2016. Automated crack detection on concrete bridges. IEEE Trans. Autom. Sci. Eng. 13, 591–599. http://dx.doi.org/10.1109/tase.2014.2354314.

Rahman, M., Liu, H., Cardenas, I.D., Starr, A., Hall, A., Anderson, R., 2021a. Towards an autonomous RIRS: Design, structure investigation, and framework. In: 2021 7th International Conference on Mechatronics and Robotics Engineering. ICMRE, pp. 164–168. http://dx.doi.org/10.1109/ICMRE51691.2021.9384846.

Rahman, M., et al., 2021b. Investigating precision and accuracy of a robotic inspection and repair system. In: SSRN Electronic Journal - Proceedings of the 10th International Conference on Through-Life Engineering Services 2021 (TESConf 2021). http://dx.doi.org/10.2139/ssrn.3945943.

Ramalingam, B., et al., 2021. Deep learning based pavement inspection using self-reconfigurable robot. Sensors 21 (2595), http://dx.doi.org/10.3390/s21082595.

Riaz, F., Rehman, S., Ajmal, M., Hafiz, R., Hassan, A., Aljohani, N.R., Nawaz, R., Young, R., Coimbra, M., 2020. Gaussian mixture model based probabilistic modeling of images for medical image segmentation. IEEE Access 8, 16846–16856. http://dx.doi.org/10.1109/ACCESS.2020.2967676.

Saifullah, S., 2020. Segmentation for embryonated egg images detection using the k-means algorithm in image processing. In: 2020 Fifth International Conference on Informatics and Computing. ICIC, pp. 1–7. http://dx.doi.org/10.1109/ICIC50835.2020.9288648.

Saleem, M., Gutierrez, H., 2021. Using artificial neural network and nondestructive test for crack detection in the concrete surrounding the embedded steel reinforcement. Struct. Concr. 22, 2849–2867. http://dx.doi.org/10.1002/suco.202000767.

Sharma, S., Phan, H., Lee, J., 2020. An application study on road surface monitoring using DTW-based image processing and ultrasonic sensors. Appl. Sci. 10 (4490), http://dx.doi.org/10.3390/app10134490.

Singh, A., Sharma, A., Mishra, R., Wagle, M., Sarkar, A., 2018. Pavement condition assessment using soft computing techniques. Int. J. Pavement Res. Technol. 11, 564–581. http://dx.doi.org/10.1016/j.ijprt.2017.12.006.

Soilán, M., Sánchez-Rodríguez, A., del Río-Barral, P., Perez-Collazo, C., Arias, P., Riveiro, B., 2019. Review of laser scanning technologies and their applications for road and railway infrastructure monitoring. Infrastructures 4 (58), http://dx.doi.org/10.3390/infrastructures4040058.

Sun, M., Pan, J., Bastard, C.L., Wang, Y., Li, J., 2019. Advanced signal processing methods for ground-penetrating radar: Applications to civil engineering. IEEE Signal Process. Mag. 36, 74–84. http://dx.doi.org/10.1109/MSP.2019.2900454.

Suzuki, T., 2023. HcFormer: Unified image segmentation with hierarchical clustering. URL: https://arxiv.org/abs/2205.09949. arXiv:2205.09949.

Torbaghan, M.E., Li, W., Metje, N., Burrow, M., Chapman, D., Rogers, C., 2020. Automated detection of cracks in roads using ground-penetrating radar. J. Appl. Geophys. 179, 104118. http://dx.doi.org/10.1016/j.jappgeo.2020.104118.

u, M.Jank˚, Stryk, J., 2017. Application of infrared camera to bituminous concrete pavements: Measuring vehicle. IOP Conf. : Mater. Sci. Eng. 236, 012104. http://dx.doi.org/10.1088/1757-899X/236/1/012104.

Wang, H., He, S., Yu, J., Wang, L., Liu, T., 2020. Research and implementation of vehicle target detection and information recognition technology based on NI myRIO. Sensors 20 (1765), http://dx.doi.org/10.3390/s20061765.

Yan, R., Kayacan, E., Chen, I., Tiong, L., Wu, J., 2019. Quicabot: Quality inspection and assessment UGV. IEEE Trans. Autom. Sci. Eng. 16, 506–517. http://dx.doi.org/10.1109/tase.2018.2829927.

Yan, H., Zhang, J., 2023. UAV-pdd2023: A benchmark dataset for pavement distress detection based on UAV images. Data Brief (ISSN: 2352-3409) 51, 109692. http://dx.doi.org/10.1016/j.dib.2023.109692.

Yeum, C.M., Dyke, S.J., 2015. Vision-based automated crack detection for bridge inspection. Comput.- Aided Civ. Infrastruct. Eng. 30, 759–770. http://dx.doi.org/10.1111/mice.12141.

Yu, H., Deng, Y., Guo, F., 2024. Real-time pavement surface crack detection based on lightweight semantic segmentation model. Transp. Geotech. 48, http://dx.doi.org/10.1016/j.trgeo.2024.101335.

Zalud, K., 2016. Image processing on raspberry pi for mobile robotics. Int. J. Signal Process. Syst. 4 (6), 494–498. http://dx.doi.org/10.18178/ijsps.4.6.494-498.

Zeng, H., Park, H., Smith, B., Parkany, E., 2017. Feasibility assessment of a smartphone-based application to estimate road roughness. KSCE J. Civ. Eng. 22, 3120–3129. http://dx.doi.org/10.1007/s12205-017-1008-9.

Zhai, C., Wang, M., Yang, Y., Shen, K., 2021. Robust vision-aided inertial navigation system for protection against ego-motion uncertainty of unmanned ground vehicle. IEEE Trans. Ind. Electron. 68, 12462–12471. http://dx.doi.org/10.1109/TIE.2020.3044802.

Zhong, M., Sui, L., Wang, Z., Hu, D., 2020. Pavement crack detection from mobile laser scanning point clouds using a time grid. Sensors 20 (4198), http://dx.doi.org/10.3390/s20154198.

Zhu, G., Nan, Z., Zhang, X., Yang, Y., Liu, X., Lin, X., 2024. High precision rail surface obstacle detection algorithm based on 3D imaging LiDAR. Opt. Lasers Eng. 178, 108206. http://dx.doi.org/10.1016/j.optlaseng.2024.108206.